BABES-BOLYAI UNIVERSITY

FACULTY OF PHYSICS

Andrada R. Stan

DOSIMETRIC ANALYSES OF MAMMOSITE MULTILUMEN (MS-ML) DEVICES IN ACCELERATED PARTIAL BREAST IRRADIATION

Doctoral Thesis Summary

Scientific Supervisor

Prof. Dr. Onuc Cozar

Cluj Napoca

2013

TABLE OF CONTENTS

INTRODUCTION

One of the main concerns in the medical world today is the continuous and aggressive rise of cancer cases every year, despite recent advances in diagnostic and treatment methods. According to the American Cancer Society (ACS) and the World Health Organization (WHO) cancer is the leading cause of death worldwide, currently with 7.6 million deaths/year, with a projected rise to 13.1 million deaths per year by the year 2030 [1,2].

The main methods to treat cancer are: surgery, radiation, chemotherapy, hormone therapy, biological therapy, and targeted therapy. For the purpose of this thesis I will focus on the treatment of cancer using radiation therapy. Specifically, the research objective of this thesis was to find an optimum device for the treatment of early stage breast cancer using High Dose Rate Brachytherapy (HDR).

Radiotherapy plays an important role in the treatment of breast cancer, and depending on the location and extent of the disease, it can be delivered as (1) External Beam Radiation Therapy (EBRT) or internally, through (2) Brachytherapy. Brachytherapy is a method of treatment that involves the irradiation of tumors by radioactive sources placed internally, resulting in a reduction of the risk of irradiation of a large area of surrounding healthy tissues. Compared to conventional EBRT, the physical advantages of brachytherapy result from a superior localization of dose to the tumor volume. Different therapeutical approaches are encountered in the field of radiation therapy, following standardized protocols and treatment schemes, based on the stage, extent of the disease, and patient preferences. Breast conserving therapy (BCT) it is the treatment of choice for the majority of women diagnosed with early stage breast cancers. As mentioned above, this procedure can be employed by using either EBRT or Brachytherapy. One method of treatment where the breast is kept intact and the dose is targeted only to the tumor and a small margin around it, is Accelerated Partial Breast Irradiation (APBI). The utilization of this technique results in shorter treatment schemes than the traditional method, with a much higher dose per fraction since only a small volume of tissue is being irradiated.

APBI has become in the last decade a popular choice in breast conserving therapy. Several studies have shown that the outcome of BCT in terms of local control and survival rates is comparable with that of modified radical mastectomy for early stage breast cancers [3-6]. In its early days, APBI was carried out as interstitial brachytherapy, a method that has

not been largely embraced by many centers, mainly due to the complexity of this procedure [7-10]. In addition, highly conformal external beam and intraoperative radiotherapy with photons and electrons were employed as APBI treatment techniques [11-14]. The following generation was represented by the MammoSite (MS) (Cytyc Corp, Marlborough, MA). Since its approval by the American Food and Drug Administration (FDA) in 2002, the use of APBI vastly increased due to the device's easy and accurate placement, less complex dose calculation and enhanced patient comfort. A number of studies described the dosimetric characteristics, reliability, safety as well as weaknesses of the MS device [15-22].

In recent years the multicatheter device concept was developed, tested and introduced in clinical practice. Strut Adjusted Volume Implant (SAVI, Cianna Medical, Aliso Viejo, CA) and Contura Multilumen-Balloon (Contura MLB, SenoRx, Inc., Irvine, CA) are probably the most popular multicatheter devices to date. A number of papers contrasted and compared the single-lumen MS device with newly designed multicatheter configurations and showed that the latter provides a greater flexibility in planning and also improvement in terms of minimizing the dose to the normal tissue [23-30].

The present research was developed in order to obtain dosimetry data to determine the best design for a new multilumen MammoSite device (MS-ML). All test devices were balloon-based multilumen brachytherapy applicators intended to be used for APBI. The devices were evaluated against the standard device dosimetric attributes and for their potential to deliver increased dosimetric flexibility. The relative dosimetric strengths and weaknesses of the different MSML design prototypes where compared for different clinical situations, dose optimization, and coverage constraints.

For this purpose ten test devices were dosimetrically evaluated. Each device was filled with a saline solution containing 5% contrast by volume, and suspended in a water phantom. The phantom containing each device was CT scanned and the obtained images were used for planning purposes. A number of 52 treatment plans were generated for two situations: first, balloon to skin distance was considered larger than 10 mm and second, balloon to skin distance larger than 5 mm, except over a continuous length of 1 cm on the surface of the skin, where this distance is 5 mm. The following parameters were evaluated using dose volume histograms (DVHs): Coverage Index (CI), Max Dose to Skin (MSD), D90, V150, V200 and External Index (EI). Three sets of plans were generated for the second scenario: maximum CI and D90 while MSD was kept below 145% of prescription; maximum CI and D90 while MSD was kept at 120% of prescription and lowest MSD while D90 is

90%. V150, V200 and EI were also kept above their limits in all instances. All of the ten test devices were able to achieve these goals, and they all proved to be a better dosimetric choice than the classic MammoSite.

CHAPTER 2

THEORETICAL ASPECTS

This chapter includes a short literature review of the theoretical aspects regarding the (1) interaction of ionizing radiation with matter, (2) a general description of brachytherapy techniques with a special accent on High Dose Rate Brachytherapy, (3) radiobiological considerations, and (4) the methods of calculation of dose distribution around linear sources, such as ^{192}Ir.

2.1. Interaction of Photons with Matter

In radiological physics there are five types of interaction of x-ray and γ-ray photons with matter. These types of interactions were largely described in extant literature over the years [31-36], however the author considered that a brief review would be beneficial. The types of interactions are: (1) Coherent scattering, (2) Photoelectric effect, (3) Compton effect, (4) Pair production and (5) Photonuclear interactions.

For this study's research purpose the Compton effect is most relevant, due to the fact that the targets are low Z materials and the photons are high energy. Therefore, only the theoretical basis of the Compton effect will be synthesized in this thesis.

2.1.1. Compton effect

In the Compton type of interaction the energy of the incident photon is transferred to an electron, after collision. The kinetics of Compton effect relates the energies and angles of the participating particles when a Compton interaction occurs. At the same rate, the probability that a Compton interaction will occur can be determined by quantum mechanical rationale [31-34].

2.1.1.1. The kinetics of Compton effect

A photon with a $h\nu$ quantum energy hits an unbound stationary electron, which is afterwards scattered with a kinetic energy K and momentum p, at an angle θ, relative to the

direction of the incident photon. After the collision the photon is scattered, with a lower energy $h\nu'$ at an angle φ, in a direction opposite to the original one. Because the electron is considered to be free, the kinematic relationships are independent of the atomic number of the medium.

In the collision kinetics both energy and momentum are conserved. Energy conservation requires that:

$$K = h\nu - h\nu' \tag{2.1}$$

This conservation of momentum along the original photon direction (0^o) can be expressed as:

$$\frac{h\nu}{c} = \frac{h\nu'}{c}\cos\varphi + p\cos\theta$$

or

$$h\nu = h\nu'\cos\varphi + pc\cos\theta \tag{2.2}$$

Conservation of momentum perpendicular to the direction of incidence gives the equation:

$$h\nu'\sin\varphi = pc\sin\theta \tag{2.3}$$

To determine *pc* in terms of kinetic energy, we have to consider the following three relativistic relationships:

$$m = \frac{m_o}{\sqrt{1-(v/c)^2}} \tag{2.4}$$

$$K = mc^2 - m_oc^2 \tag{2.5}$$

$$p = mv \tag{2.6}$$

In the above equations m is the electron's relativistic mass, *v* is its velocity, *m* is its mass and *p* is its momentum.

Therefore, *pc* can be written in terms of *K* in Eq (2.2) and (2.3) :

$$pc = \sqrt{K(K+2m_oc^2)} \tag{2.7}$$

in which m_o is the electron's rest mass.

By substituting *pc* in Eq. (2.2) and (2.3) we obtain:

$$h\nu = h\nu' \cos\varphi + \sqrt{K(K + 2m_o c^2)}\cos\theta \tag{2.8}$$

$$h\nu' \sin\varphi = \sqrt{K(K + 2m_o c^2)}\sin\theta \tag{2.9}$$

Furthermore, by resolving the system of above equations, we obtain the energy of the scattered photon as:

$$h\nu' = \frac{h\nu}{1 + (h\nu / m_o c^2)(1 - \cos\varphi)} \tag{2.10}$$

$$\cot\theta = \left(1 + \frac{h\nu}{m_o c^2}\right)\tan\left(\frac{\varphi}{2}\right) \tag{2.11}$$

Which is one solution of the kinematics of Compton interactions [33-34].

2.1.1.2. Probability of Compton interactions

The probability of Compton interactions was first introduced by J.J. Thomson. In his theory Thomson considered the free electron oscillating under the influence of the electric vector of an incident electromagnetic wave. Following this elastic scattering, the electron retains no kinetic energy and it releases a photon of the same energy.

The differential cross section per electron for a photon scattered at an angle φ, per unit solid angle, could be expressed as:

$$\frac{d_e\sigma_o}{d\Omega_\varphi} = \frac{r_o^2}{2}\left(1 + \cos^2\varphi\right) \tag{2.12}$$

in typical units of cm^2 sr^{-1} per electron. $r_o = e^2/m_o c^2 = 2.818 \times 10^{-13}$ cm is called the "classical electron radius".

The total Thomson scattering cross section per electron, ${}_e\sigma_o$, can be obtained by integrating Eq. (2.12) over all directions of scattering. This will be simplified by assuming cylindrical symmetry and integrating over $0 \le \varphi \le \pi$, noting that the annular element of solid angle is given in terms of φ by $d\Omega_\varphi = 2\pi \sin\varphi \, d\varphi$:

$$\sigma_o = \int_{\varphi=0}^{\pi} d_e\sigma_o = \pi \cdot r_o^2 \int_{\varphi=0}^{\pi}\left(1 + \cos^2\varphi\right)\sin\varphi \cdot d\varphi =$$

$$= \frac{8\pi \cdot r_o^2}{3} = 6.65 \times 10^{-25} \text{ cm}^2/\text{electron} \qquad (2.13)$$

In Thomson's theory the value of 6.65×10^{-25} cm^2/e was considered to be too large for $h\nu > 0.01$ MeV.

Following Thomson's theory, Klein and Nishina applied Dirac's relativistic theory of the electron to the Compton effect. Their goal was to obtain an improved cross section [34].

According to Klein and Nishina the differential cross section for photon scattering at angle φ, per unit solid angle and per electron can also be written in the following form:

$$\frac{d_e\sigma}{d\Omega_\varphi} = \frac{r_o^2}{2}\left(\frac{h\nu'}{h\nu}\right)^2\left(\frac{h\nu}{h\nu'} + \frac{h\nu'}{h\nu} - \sin^2\varphi\right) \qquad (2.14)$$

2.1.1.3. Dependence of Compton effect on energy and atomic number

During a Compton interaction the incident photon transfers part of its incident energy to a free electron in the attenuating medium. The energy of the incident photon is therefore large compared to the binding energy of the electron. When the energy of the incident photon increases beyond the binding energy of the loosely bound electron, the Compton effect becomes more and more important [31,34,36]. Due to the fact that the electrons of the attenuating medium, involved in the Compton interaction are loosely bound (free), its mass attenuating coefficient (σ/ρ) is independent of the atomic number Z, and depends only on the number of electrons per gram [35,36]. It was demonstrated that in the range of photon energies used in radiotherapy, the Compton effect is the most relevant mode of interaction of the photons with the absorbing medium [31,33-36]. Also, in the region where the Compton effect is the only possible mode of interaction, the same attenuation of the beam will occur in any material of equal density thickness [35,36].

2.2. Brachytherapy – General Concepts

Historically, brachytherapy was described as a treatment with small-sealed radioactive sources at a short distance from the target volume. Initially, the small

encapsulated sources used in the treatment of malignant tumors were radium and radon sources. Afterwards, Cs-137, Ir-192, Au-198, Pd-103 and I-125 started to be used with this method of treatment. This was due to their superiority over radium sources, in terms of energy, source size, flexibility, half-life and potential radiation hazards to the hospital personnel [36,37]. The concern regarding the radiation hazard was increasing in the 1950s, phenomenon that led to a substantial decrease in the use of brachytherapy [37].

The principle of afterloading technique was introduced around that time to address the concerns related to the harmful effects of radiation during brachytherapy treatments. The new technique was carried out by inserting open empty applicators in the tumor, and then these were loaded with radioactive sources [37-40]. In the past brachytherapy played an important role in the management of cancers of several localizations, including brain, head and neck, uterine cervix, prostate and endometrium, in recent years the treatment of breast tumors became popular as well [41, 42].

2.2.1. Brachytherapy source specification

Traditionally the source strength was expressed in terms of activity. Since the sources are encapsulated, the materials used for encapsulation attenuate and scatter the emitted photons, the result being that the energy fluence will be altered. This is the reason why more ways to specify a source strength were introduced: exposure rate at a specified distance, equivalent mass of radium, apparent activity or air kerma strength [33-35, 44-48]. The current recommendation by the American Association of Physicists in Medicine is to use air kerma strength for source specification.

2.2.2. Dose calculation formalism

AAPM task group 43 and the subsequent updates [44,47,48] developed a dose calculation formalism for the dosimetry of interstitial brachytherapy sources, in which the source strength is expressed in terms of air kerma strength S_k. In this formalism the tissue attenuation factor is replaced by the radial dose function, g (r), the anisotropy of dose distribution is described by the anisotropy function, F (r,θ), and the exposure rate constant has been replaced by the dose rate constant, Λ. In the calculation formalism developed by AAPM in 1987 and updated in 2004 [44,47], the dose rate at a point with coordinates (r,θ) from the center of a source can be expressed as:

$$\dot{D}(r,\theta) = S_k \Lambda \frac{G(r,\theta)}{G(1,\pi/2)} F(r,\theta)\, g(r) \qquad (2.15)$$

Where: S_k is the air kerma strength (U) of the source ; Λ is the dose rate constant (cGy h^{-1} U^{-1}); r is the radial distance (cm) of a point of interest from the source center; θ is the polar angle (radian) formed by the longitudinal axis of the source and the ray from the source center to the point of interest; G(r,θ) is the geometry function (cm^{-2}) that describes inverse square falloff and accounts for the distribution of the radioactive material ; F(r,θ) is the anisotropy function that accounts for angular dependence of dose due to absorption and scatter by the encapsulation and the medium, is dimensionless, and is equal to unity on the transverse axis ; g(r) is the radial dose function that accounts for radial dependence of dose on the transverse axis due to photon absorption and scatter in the medium, is dimensionless, and is equal to unity at 1 cm on the transverse axis.

Figure 2.1. illustrates the dose rate at a point with coordinates (r,θ) from the center of a source.

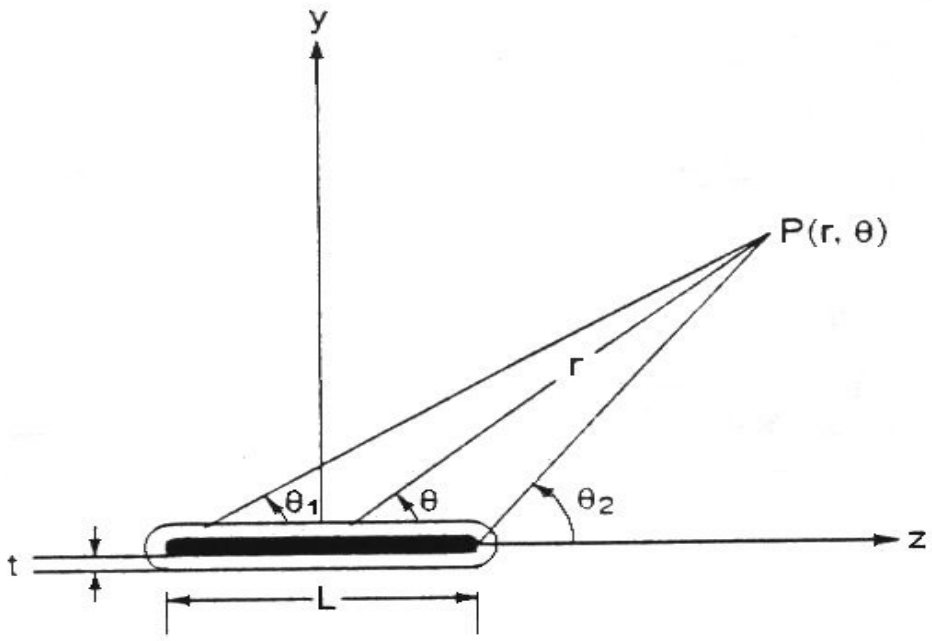

Figure 2.1. Schematic diagram illustrating the geometry of a dose calculation formalism for a linear radioactive source.

2.3. High Dose Rate Brachytherapy – General Aspects

The use of remote afterloaders provides the ability to irradiate tumors at a variety of dose rates, from high dose rate to conventional low dose rate. Since the method of testing

used in this project utilized High Dose Rate Brachytherapy (HDR), only the characteristics related to this method of treatment are presented in the following pages.

2.3.1. Radiobiological concepts

Although there are several advantages of HDR over LDR [44,49,51], the biggest controversies over the two techniques of dose delivery, were related to the radiobiological effects. It was demonstrated, that the dose-rate effect is greater for normal cells than for tumor cells and this is the reason why the fractionation and dose-rate are playing major roles in both external beam radiation therapy and brachytherapy [51-55]. Based on this theory, in order to obtain comparable clinical results with HDR as with LDR, the dose per fraction and fractionation needed to be increased.

2.3.1.1. The linear quadratic model

Historically, the comparison between LDR and HDR was done by the application of the Linear Quadratic Model (L-Q model). In this model the biologically effective dose [56] (BED) is expressed as:

$$BED = -(\ln S.F.) / \alpha = NRt [1 + G \times Rt / (\alpha/\beta)] - kT \qquad (2.16)$$

Where: S.F. is the cell surviving fraction; N is the number of fractions; R is the dose rate expressed in Gy/h; t is the time for each fraction; T is the overall time, expressed in days, available for repopulation; α, β are tissue specific parameters, with α relating to the initial slope of the cell survival curve, and β defining its curviness; α/β is the dose in Gy for which α and β are equal [53]; G is a function of the irradiation time, the dose rate, the cellular repair and time between fractions.

2.3.2. High Dose Rate unit description and source calibration

The HDR remote afterloading device uses one single ^{192}Ir source, of high activity. The choice of ^{192}Ir as the radioisotope of preference for HDR afterloaders, was based on the radioisotope's small dimensions, due to its high specific activity, and low photon energy. The ^{192}Ir source is a small linear source embedded at one end of a flexible cable, called the source wire. This source wire is placed in a shielded safe inside the HDR unit and is extended, travelling automatically from the storage space and into the applicators during treatment. The design of the HDR unit includes several channels, through which the source is retracted

or extended in a sequential manner. A computer controls the transit of the source wire remotely. The source wire travels from the safe, through the unit's channels into the transferring tubes and finally in the applicators that are placed into the tumor. The ^{192}Ir source has a half-life of 73.82 days with a rate of decay of 1%/day, so it needs to be replaced every 3 to 4 months to ensure an optimum rate of dose delivery [57]. After the source is installed, a series of tests are performed, among them mechanical and safety checks which are testing HDR unit's response to emergency situations, positioning accuracy and reproducibility.

In Radiotherapy one of the most important tasks for a medical physicist is patient specific quality assurance (QA) [58,59]. One of the most important steps is the source calibration.

The calibration of ^{192}Ir sources is routinely performed using a well-type re-entrant ionization chamber. One type of a well-type ionization chamber is filled with air and communicates to the outside air through a vent hole. The chamber has an outer shell of conductive material with walls that are forming an inner well disposed within and electrically connected to the outer shell [60,61]. The active volume of the chamber is big enough to give an optimum ionization current that is measured with an electrometer. The value of air kerma strength can be determined from the measurement of the ionization current produced by the ^{192}Ir source in the ionization chamber, corrected for pressure, temperature and ion recombination at the time of source and chamber calibration [35,60]:

$$S_k = I \times C_{T,P} \times N_{el} \times N_c \times A_{ion} \times P_{ion} \qquad (2.17)$$

where: I is the current reading, expressed in nA; $C_{T,P}$ is the correction for temperature and pressure; N_{el} is the electrometer calibration factor; N_c is the chamber calibration factor; A_{ion} is the ion recombination correction factor at the time of chamber calibration; P_{ion} is the ion recombination correction at the time of source calibration.

2.3.3. High Dose Rate Brachytherapy dose calculation

Computer Tomography (CT), Magnetic Resonance Imaging (MRI) and Ultrasound techniques (US), are the imaging modalities that allow a full 3D anatomy reconstruction, dose calculation and isodose distribution [62-64]. These methods are the standard of practice in imaging for planning in external beam radiation as well as brachytherapy [65,66]. The recommended dose calculation formalism for point and linear sources is AAPM's TG-43

[44,47]. Following this formalism, the dose rate at a given distance r in the medium is given by the following equation:

$$D(r) = \Lambda S_k [g(r)/ r^2] \varphi_{an} \quad (2.18)$$

where: Λ is the dose rate constant for the source; g(r) is the radial dose function; φ_{an} is the average anisotropy factor; r is the distance in the medium, for which the dose rate is calculated, and is measured from the center of the source at each dwell position.

The most effective method to analyze the dose distribution in the irradiated volume is done using dose-volume histograms (DVH's) [67,68]. These are the consecrated helpful tools in evaluating plans for individual patients. They are particularly useful in assessing dose uniformity and the degree to which normal tissue is irradiated. DVH's can facilitate the brachytherapy planning process. The DVH is the starting point for calculation of tumor control probabilities and normal tissue complication probabilities.

CHAPTER 3

DOSIMETRIC ANALYSES TO DETERMINE THE OPTIMAL DESIGN FOR MAMMOSITE MULTILUMEN (MS-ML) DEVICES

3.1. Device description and selection

Ten prototype balloons were evaluated for dosimetric characteristics. All test devices are 4-5 cm variable diameters spherical, multilumen polyurethane balloons with 3 mm lumen center to balloon shaft center spacing (test devices 1-5), and 2 mm lumen center to balloon shaft center spacing configurations (test devices 6-10). The cross-sections of the devices are presented in Figure 3.1.

3.2. Equipment

In addition to the ten test articles previously described, the following equipment was also used in our attempt to determine the optimum device to be used for APBI, and also to provide the users with the best selection of dummy wires, imaging and planning techniques. The CT scanner used in this study was an 8 slice GE discovery CT Scanner. All treatment plans were created and optimized using a Varian BrachyVision Treatment Planning System – Brachytherapy Planning Software (Version 8.2).

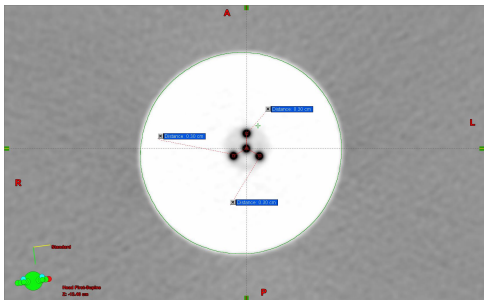

Test Device 1

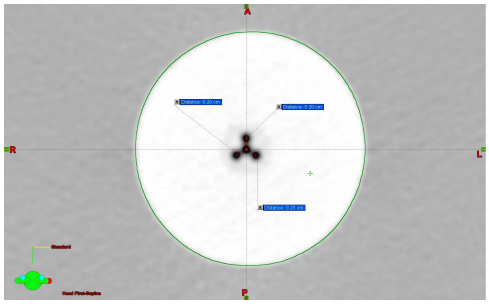

Test Device 6

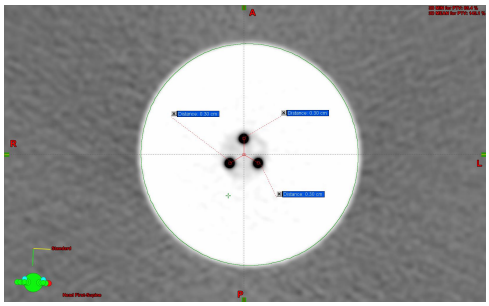

Test Device 2

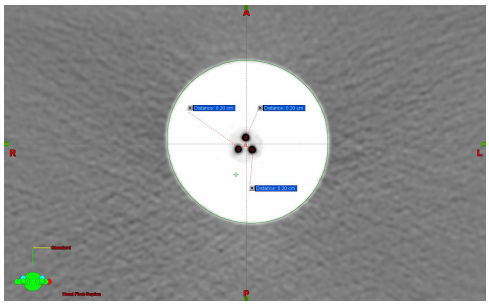

Test Device 7

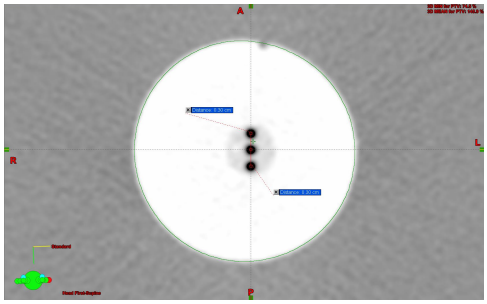

Test Device 3

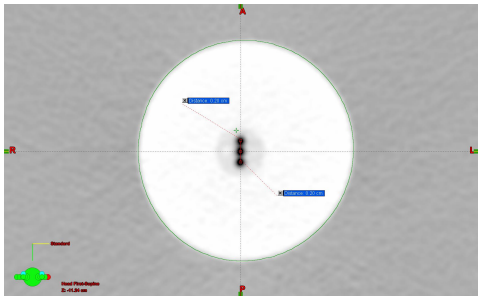

Test Device 8

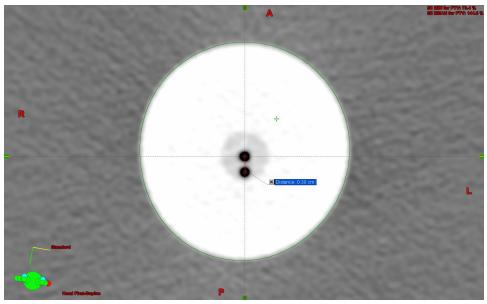

Test Device 4

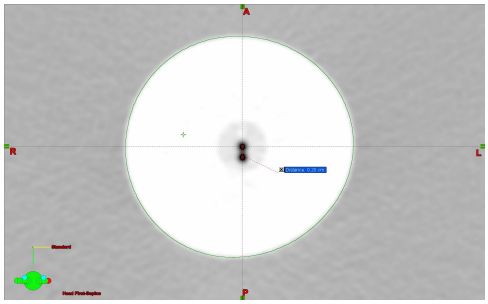

Test Device 9

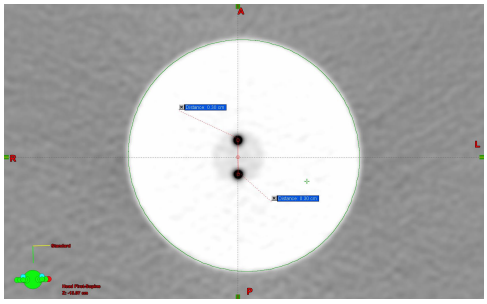

Test Device 5

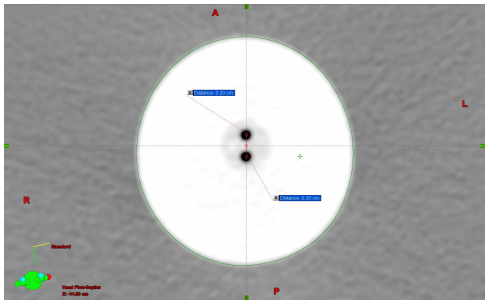

Test Device 10

Figure 3.1. Cross-section of test devices

An in-house made water bath imaging phantom and a CT compatible positioning system designed to keep the test article's long axis perpendicular to the scanning plane were used. The solution used to inflate the balloons was Optiray 350 Contrast Solution (Ioversol Injection 74% 350mg/ml Organically Bound Iodine) - with a 5% concentration by volume in 0.9% saline solution.

3.3. Treatment Planning Technique

The CT images were exported to the BrachyVision Planning Station (Varian Medical Systems, Inc, Varian Oncology Systems, Charlottesville, VA). Each test device was evaluated in axial and multiplanar reconstruction views for skin spacing, symmetry and conformance of the applicator. All the structures created were theoretical, simulating all potential clinical conditions.

3.3.1. Contouring and structure definition

The Body structure was automatically reconstructed by the BrachyVision software following the import of CT studies into the system. Several structures associated with the device and with the hypothetical surrounding healthy tissue were created for prescription and optimization and they are reported as follows. For each device studied the Body represents the body contour when the distance between the balloon surface and the skin surface is larger than 10 mm. Body 1 represents the body contour when the distance between the balloon surface and the skin surface is larger than 5 mm except over a continuous length of 1cm on the surface of the skin, were this distance is 5 mm and 1 lumen is oriented toward the skin. Following the same pattern, Body 2 represents the body contour when the distance between the balloon surface and the skin surface is larger than 5 mm except over a continuous length of 1 cm on the surface of the skin, were this distance is 5 mm and 2 lumens are oriented toward the skin (where applicable). MammoSite (MS) represents the actual reconstructed balloon of the test device. MS+1+Opt represents the actual balloon plus 1 cm margin in all directions when the distance between the balloon surface and the skin surface is larger than 10 mm (Body) and it is used to generate other structures and for volume optimization at its surface. In the same fashion MS+1+Opt1 and MS+1+Opt2 represent the actual balloon plus 1 cm margin in all directions, except over the continuous length of 1 cm on the surface of the skin, were this distance is 5 mm and 1 lumen is oriented toward the skin (Body 1), respectively 2 lumens are oriented towards the skin (Body 2). The Planning Target Volume (PTV) was generated as a uniform layer of 1cm around the MS structure when the distance

between the balloon surface and the skin surface is larger than 10 mm (Body). Subsequently PTV1 and PTV2 were created as a uniform layers of 1 cm around the MS structure except over the continuous length of 1 cm on the surface of the skin, were this distance is 5 mm and 1 lumen is oriented toward the skin (Body1), 2 lumens respectively (Body 2). Healthy Breast tissue was created as a 2 cm layer around the PTV when the distance between the balloon surface and the skin surface is larger than 10 mm. In the same fashion Healthy Breast 1 and 2 were created in direct correlation to the definition of Body 1 and Body 2. The structures created for optimization purposes are presented in Figure 3.2.

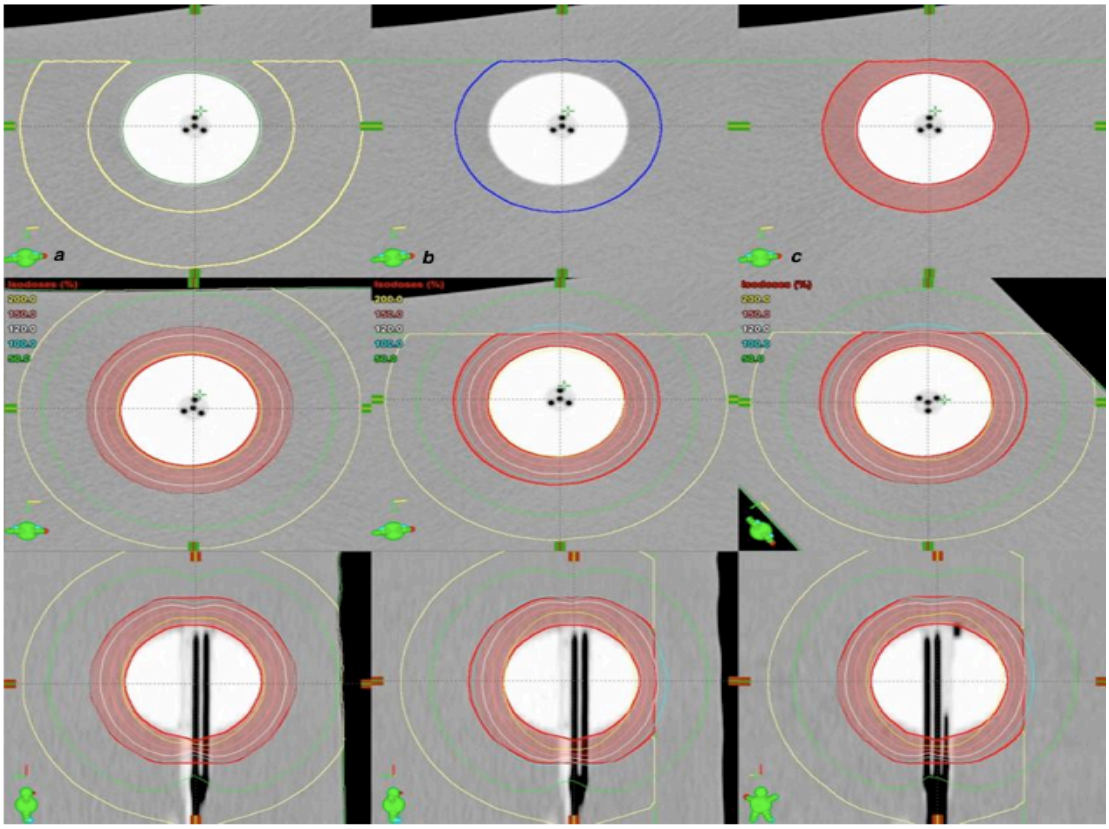

Figure 3.2. Structures created for optimization purposes: a) represents the Healthy Breast structure; b) represents the MS+1+Opt structure and c) represents the PTV.

3.3.2. Dose prescription and optimization

The prescription was 340 cGy per fraction to the surface of PTV, PTV1 and PTV2. The planning criteria applied in these cases followed the National Surgical Adjuvant Breast and Bowel Project B-39/Radiation Therapy Oncology Group 0413 [69] guidelines for APBI irradiation with respect to D90, V100, V150, V200, V300 and MSD. D90 represents the percentage of the prescribed dose delivered to 90% of the PTV. MSD is the Maximum Skin Dose, V150, V200 and V300 represent the volumes (cc) covered by the percentage (%) of the

dose. Wazer et al. [70] first showed in their paper that escalated values for these entities are linked to the development of fat tissue necrosis. Lately, several authors [27-29,41,42,68] analyzed early tolerances and late toxicities related to these dosimetric parameters.

The Coverage Index (CI) is a measure of the fraction of the breast target volume receiving a dose equal to or greater than the prescribed dose, i.e. V100 expressed in %.

The External Index (EI) was calculated by dividing the volume of Healthy Breast that is receiving at least 340cGy/fraction (in cc) by the total volume of the whole breast volume, expressed in %. The planning criteria are presented in Table 3.3.

$$EI = \frac{\text{Volume (cc) of Healthy Breast receiving 340 cGy/fx}}{\text{Total Volume (cc) of Healthy Breast and PTV}}$$

The planning criteria are presented in Table 3.1.

Planning Criteria	D90	V150	V200	MSD	CI	EI
1	>90%	≤ 50cc	≤ 10cc	≤ 145%	High	≤ 5%
2	>90%	≤ 50cc	≤ 10cc	≤ 120%	≥ 90%	≤ 5%
3	=90%	≤ 50cc	≤ 10cc	Low	-	≤ 5%

Table 3.1: Planning criteria

Three potential clinical situations were considered during the planning process. (a) each device has an arbitrary position in the tissue and the minimum skin and chest wall spacing is equal or greater than 10 mm; (b) one catheter being oriented toward the skin, with a minimum skin spacing of 5 mm for 1 cm^2 and a minimum chest wall spacing equal or greater than 10 mm; (c) two catheters were oriented toward the skin with a minimum skin spacing of 5 mm for 1 cm^2 and a minimum chest wall spacing equal or greater than 10 mm. Depending on the device's design, two or three sets of plans were created for each of the scenarios described above. A total of 52 dosimetry treatment plans were developed. The isodose distribution for all the plans was obtained by volume optimization of the MS+1cm+Opt structures, followed by slight manual adjustments. All the plans generated for each of the situations described above were evaluated by means of dose volume histogram (DVH) analysis.

3.4. Results and Discussions

For all devices and clinical situations described in this study the PTV volumes were found to be between 78.8 cc and 86.7 cc with a mean value of 81.95 cc and standard deviation of 2.06.

One set of plans was optimized for high Coverage Index (CI) and high D90, with a Max Skin Dose less than 145% (493cGy), EI ≤5%, V150≤50cc and V200≤10cc. Relevant details are listed in Table 3.2.

Device #	Device position	MSD (cGy)	CI (%)	EI (%)	D90 (%)	V150 (cc)	V200 (cc)
1	1 cts[a]	455.1	98.4	0.493	106.0	31.0	8.6
1	2 cts	466.0	98.4	0.695	106.5	31.5	8.9
2	1 cts	455.9	99.0	0.592	106.5	31.0	8.9
2	2 cts	464.7	99.0	1.092	107.8	32.1	9.6
3	1 cts	455.8	95.7	1.586	106.1	31.5	9.6
4	1 cas[b]	430.1	97.6	1.218	107.3	31.3	8.7
5	1 cts	475.1	95.2	0.764	104.6	2.5	8.3
6	1 cts	456.6	98.4	0.558	106.1	31.0	8.4
6	2 cts	469	98.4	0.468	105.9	31.0	8.4
7	1 cts	449.1	97.5	0.335	104.9	29.9	7.6
7	2 cts	451.1	97.5	0.868	106.3	31.2	8.6
8	1 cts	449.4	97.5	1.170	107.1	31.2	8.5
9	1 cas	472.4	96.5	0.942	105.8	31.2	8.5
10	1 cts	449.6	96.5	0.372	104.4	30.0	6.9

[a]cts - catheter toward skin [b]cas – catheter away from skin

Table 3.2 : Results of plan optimization for high CI, high D90 & Max Skin Dose < 145% when the minimum skin spacing is 5mm

For all clinical situations the MSD was kept under 493 cGy with a maximum value of 475.1 cGy for the test device #5, planned with 1 catheter towards the skin. The Coverage Index was well above 90% with a minimum of 95.2% for the test device #5. For all the clinical situations the External Index was below 5% with a maximum of 1.586% for the test device #3 and the plan developed with 1 catheter toward the skin. More than 100% of prescription dose delivered to 90% of the PTV was obtained for all three clinical situations. As we expected, V150 and V200 were kept below 50 cc's respectively 10 cc's, for all dosimetric plans created for these dose constraints.

The second set of plans was developed having less than 120% (408 cGy) MSD and high D90, CI≥90%, EI≤5%, V150≤50cc and V200≤10cc as main optimization goals. The results are listed in Table 3.3.

Device #	Device Position	MSD (cGy)	CI (%)	EI (%)	D90 (%)	V150 (cc)	V200 (cc)
1	1 cts[a]	408	90.7	0.308	100.5	26.5	6.6
1	2 cts	407.9	93.2	1.140	103	29.5	8.8
2	1 cts	407.9	92.8	0.179	101.9	26.6	6.5
2	2 cts	407.9	93.2	1.329	103.1	29.2	8.7
3	1 cts	408	93.0	1.680	103.2	30	9.5
4	1 cas[b]	407.8	94.2	0.511	103.4	27.9	7.0
5	1 cts	408.0	91.9	1.208	102.0	28.3	8.4
6	1 cts	407.9	94.3	0.404	103.1	28.2	7.4
6	2 cts	408.0	94.7	1.511	104.7	31.0	9.3
7	1 cts	407.9	93.1	0.381	102.2	27.6	6.7
7	2 cts	407.9	93.4	0.968	103.3	29.2	8.4
8	1 cts	407.8	93.8	1.241	103.9	29.1	8.0
9	1 cas	408.0	91.6	0.852	101.4	28.1	7.8
10	1 cts	407.9	96.3	0.557	104.6	30.0	7.6

Table 3.3: Results of plan optimization for high D90 & Max Skin Dose ≤ 120% when the minimum skin spacing is 5mm

Analyzing Table 3.3 we can see that it was possible to keep the MSD below 120% from the prescription dose and still achieve an optimal CI as well as a high D90. The MSD of 408 cGy and the lowest CI of 90.7% were obtained for test device #1 in the scenario with one catheter toward the skin. In all situations EI, V150, V200 were well below 5%, 50 cc's and 10 cc's respectively. D90 was more than 100% for all the devices and clinical situations considered for the present study.

The idea of creating a third set of plans was to demonstrate that even in the most challenging clinical situations (i.e. distance to skin of 5 mm in more than 3 slices, which with the simple MS device was considered an exclusion criteria) we can still achieve a small skin dose while maintaining the criteria described in Table 3.1. Table 3.4 reflects the results obtained for plans optimized for 90% D90 and low skin dose.

Device #	Device Position	MSD (cGy)	CI (%)	EI (%)	D90 (%)	V150 (cc)	V200 (cc)
1	1 cts[a]	359.8	74.9	0.060	90.0	18.4	4.7
1	2 cts	325.4	79.7	1.330	90.0	23.9	8.6
2	1 cts	338.6	74.2	0.039	90.0	17.8	4.2
2	2 cts	317.4	80.0	1.735	90.0	24.4	9.3
3	1 cts	332.1	78.9	0.444	90.0	21.0	6.6
4	1 cas[b]	311.0	80.5	1.447	90.0	24.5	8.7
5	1 cts	324.2	79.2	0.818	90.0	21.8	7.2
6	1 cts	345.4	75.2	0.096	90.0	18.6	5.1
6	2 cts	326.8	77.5	0.103	90.0	20.5	6.4
7	1 cts	348.2	75.4	0.189	90.0	18.7	5.3
7	2 cts	339.2	75.5	0.102	90.0	19	5.2
8	1 cts	331.4	76.2	0.131	90.0	18.7	4.6
9	1 cas	344.1	77	0.241	90.0	19.8	5.8
10	1 cts	334.6	75.0	0.200	90.0	19.0	5.2

Table 3.4: Results of plan optimization for 90% of D90 and Low Skin Dose when the minimum skin spacing is 5mm

In all instances presented in Table 3.4 the dose to the skin was low, even for the situations where the distance to the skin was 5 mm and the catheters were oriented toward skin. D90 was equal to 90% for all cases and EI, V150 and V200 were kept below their limiting values.

For the situation when the devices have an arbitrary position in the phantom (tissue) and the minimum skin and chest wall spacing is at least 10 mm all the optimization goals described in Table 3.1 are successfully met by all the balloons studied. As expected, the MSD was kept below 100% of the prescription dose. The CI was above 95% for all situations with a minimum of 95.2 % and a max of 99% having a mean value of 97.54% and standard deviation of 1.18. The EI was kept well below 5% for all devices with a minimum of 0.263% and a max of 1.586%. D90 was above 104% for all the cases. V150 was found to be below 50cc with a maximum value of 32.1 cc and V200 was kept below 10cc without any difficulty.

As all test devices were able to achieve the goals of this study, it is difficult to dosimetrically rank them, especially since their asymmetry is different. However, after taking into account all the planning aspects, the flexibility and complexity of the dose optimization for any clinical situation, we can state that test device #1 has the best configuration among all ten devices tested. Its configuration with 3 mm offset of the lumen center to balloon shaft center can achieve a more off-center dose coverage in practice. Another notable attribute of test device #1 is the fact that it can achieve a dose shift in multiple planes, compared to the other devices tested which can achieve a dose shift only in one plane (test device #3) or none at all.

This study contributes to extant literature by bringing further proof that a multilumen design provides more flexibility in patient selection, planning and dosimetric outcome [71]. The possibility of planning with all or just a few of the lumens offers a better control of the dose distribution with significantly lower dose at the skin, chest wall and lung level [27-29,71].

CHAPTER 4

DETERMINATION OF THE CLINICAL SUITABILITY OF A 23 CC INFLATED MS-ML BALLOON

There are certain clinical situations when the use of a balloon type device faces geometrical limitations (i.e. small breasts, tumor is located too close to the skin and/or the chest wall). In an attempt to address and overcome such issues we developed a parallel study in order to obtain dosimetric data that characterizes the MammoSite-Multilumen (MS-ML) containing only 23cc of fluid.

4.1. Planning Technique

Eight scenarios were considered for planning, assuming that the closest distance to the skin and to the chest wall were in a plane orthogonal to the MS-ML lumens and passing through the center of the MS-ML balloon.

A total of 16 plans were generated, 8 plans for each of the 2 situations: the plastic (non-tissue) areas located outside the balloon and containing the catheters (tip and shaft) were subtracted or not from the PTV. The thickness of the PTV considered was 3, 5 and 10mm toward the skin and 3, 5 and 10mm toward the chest wall. The chest wall was assumed to be directly opposed to the skin. The thickness of the PTV on the perpendicular to the skin to chest wall direction was 5, 7 and 10mm.The thickness of the PTV at the lumens ends of the balloon was always as 10mm.

The following parameters were evaluated using DVHs: PTV size; Max Skin Dose; Max Chest Wall Dose; V100, V95, V90, D90, V150, V200, V300 and Min, Max and Mean Dose in the PTV.

All 16 plans were designed to achieve the NSABP B-39/ RTOG 0413 protocol requirements for treatment, even though in some scenarios the evaluation parameters were close to the edge of acceptability.

4.1.1. Structure reconstruction and definition

Planning for small breast patients can be challenging sometimes due to the device's proximity to the skin and chest wall and it was an exclusion criteria for balloon based Accelerated Partial Breast Irradiation in the past [69,70,72]. In an effort to overcome this

issues we created several optimization structures to aid in the planning process, offering a greater flexibility in dose prescription and optimization. We started with the reconstruction of the MS-ML balloon and we found that the total volume was 25.6cc: 23cc fluid and 2.6cc central catheter volume.

MS+1cm represents the actual balloon plus a variable margin in 6 directions for a total of 8 scenarios. The margin toward the tip and the shaft of the balloon was 10mm. We considered three potential clinical situations in creating the margins towards the skin, chest wall, and at +/- 90deg left and right of the balloon. So, the margin for the MS+1 around the MS-ML balloon toward the skin and chest wall was considered 3, 5 and 10mm, while towards left and right was 5, 7 and 10mm each at a time. We also contoured the tip and the shaft of the balloon as they will play a role in the generation of one of the PTV volumes. The PTV Evl structure was created following the NSABP B-39/ RTOG 0413 [69] definition by subtracting the MS-ML from the MS+1 structure as we can see in Figure 4.1.

Based on the NSABP B-39 / RTOG 0413 protocol definition, the PTV Evl has to be generated as the volume of breast tissue surrounded by the uniform expansion of the balloon radius in all dimensions by 1 cm minus the balloon volume [69].

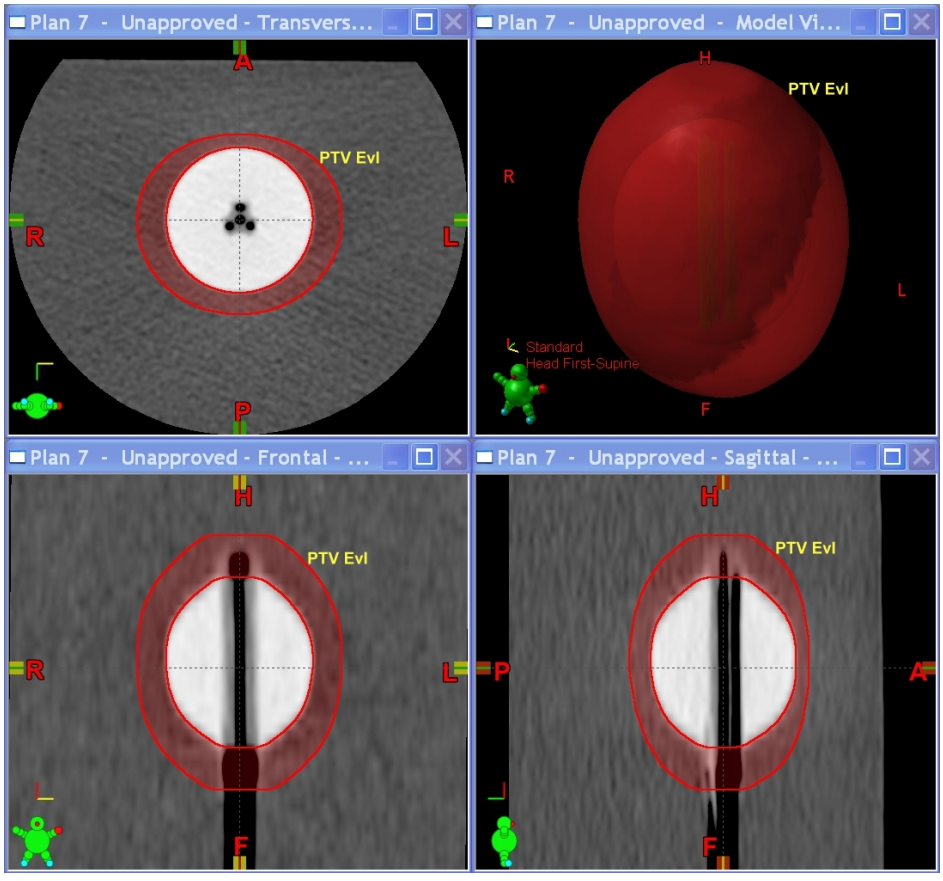

Figure 4.1. The PTV Evl structure

At this reconstruction stage I considered that it would be highly appropriate to introduce a new PTV structure, which will be used for dose prescribing and reporting. PTV Est is the PTV Evl structure from which the Tip structure and the Shaft structure were subtracted. PTV Est structure is represented in Figure 4.2.

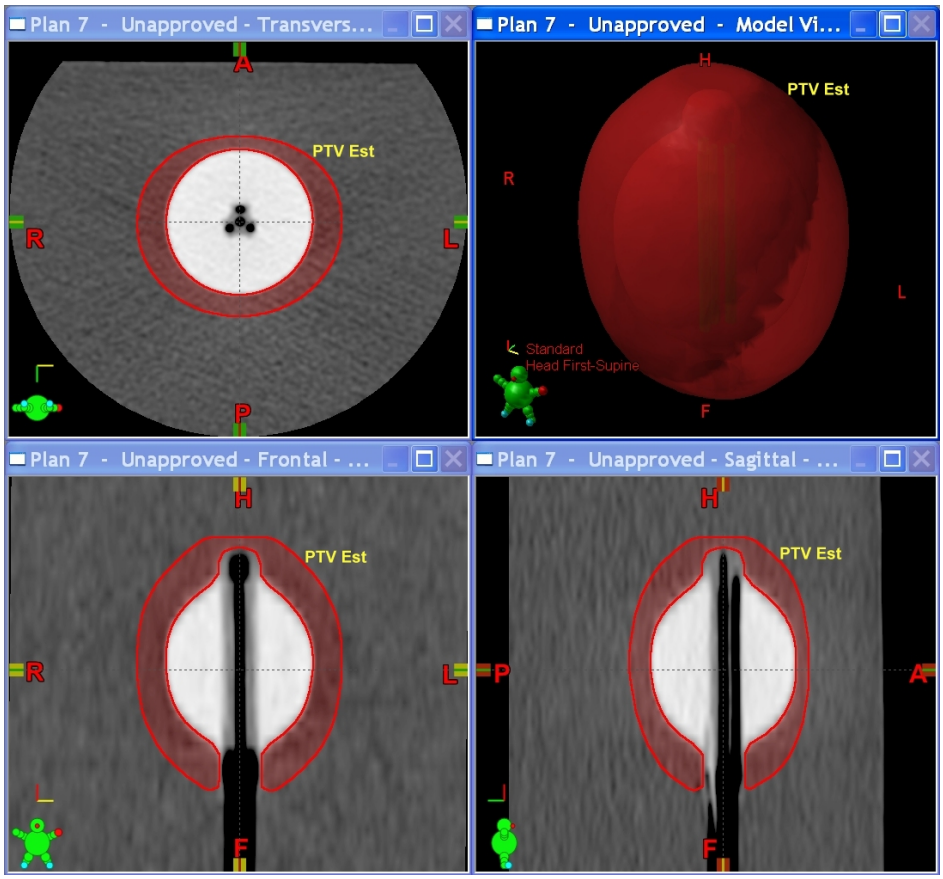

Figure 4.2. The PTV Est structure

Two new optimizing structures were created for the purpose of determining a structure designed to contain the Max Skin Dose, Max Chest Wall Dose respectively. The Max Skin structure has at least 8 cm^2 of its surface common with the anterior side of the MS+1cm structure. The Max Chest Wall structure has at least 8 cm^2 of its surface common with the posterior side of the MS+1cm structure. Both newly created structures are at least 8mm thick.

4.1.2. Dose prescription and optimization

The author tried to generate all possible clinical situations, including the most challenging scenarios, when the distance to the skin and / or the chest wall would be a limiting factor with other types of devices. Following the NSABP B-39 / RTOG 0413

protocol recommendation [69] the prescription dose used was 340cGy to the outer surface of PTV (Evl or Est), for all the plans generated in this study. All the doses reported for all the structures created in this study are based on this nominal prescription of 340 cGy.

The thickness of the PTV (Evl or Est) in the 6 main directions for each plan as well as the MS-ML lumens orientation is shown in Table 4.1.

Plan #	**PTV thickness toward the**				**MS-ML lumens orientation**
	Skin (mm)	**CW (mm)**	**(+)90^o & (-)90^o from Skin (mm)**	**Shaft & Tip (mm)**	
1	10.0	10.0	10.0	10.0	arbitrary
2	5.0	5.0	5.0	10.0	arbitrary
3	3.0	3.0	10.0	10.0	1 catheter toward skin
4	3.0	3.0	7.0	10.0	1 catheter toward skin
5	3.0	3.0	5.0	10.0	1 catheter toward skin
6	3.0	5.0	10.0	10.0	1 catheter toward skin
7	3.0	5.0	7.0	10.0	1 catheter toward skin
8	3.0	5.0	5.0	10.0	1 catheter toward skin

Table 4.1: PTV thickness and lumens orientation

The number of lumens used, number of radiation source positions and size of the dwell times were chosen in such a fashion to deliver optimal dose coverage of the target volume while following the subsequent optimization goals:

Planning Criteria	D90	V90	V95	V100/CI	V150	V200	V300	MSD	MCWall
	>90% of the Rx Dose	>90% of the PTV	>85% of the PTV	>80% of the PTV	≤ 50cc	≤ 10cc	≤ 1cc	≤ 120%	≤ 120%

Table 4.2: Planning criteria

4.2. Results and Discussions

The isodose distribution, the maximum Dose to the Skin and the Maximum Dose to the Chest Wall are similar in these 2 cases; the PTV is not the same and then all the parameters

calculated as reference to them are not identical (PTV volume,V100, V95, V90, D90, V150, V200, V300, Min, Max and Mean Dose in the PTV).

Based on volume optimization the results from DVH analysis are summarized in the following 4 tables: 4.3.A, B, C, and D:

Plan #	PTV thickness toward the				MS-ML lumens orientation	MS-ML Properties				PTV Est Volume (cc)
	Skin (mm)	CW (mm)	(+)90° & (-)90° from Skin (mm)	Shaft & Tip (mm)		Long Axis (cm)	Main Diameters 1 (cm)	Main Diameters 2 (cm)	Volume (cc)	
Limit						*N/A*	*N/A*	*N/A*	*N/A*	*N/A*
1	10.0	10.0	10.0	10.0	arbitrary	4.10	3.44	3.43	25.6	70.3
2	5.0	5.0	5.0	10.0	arbitrary	4.10	3.44	3.43	25.6	38.8
3	3.0	3.0	10.0	10.0	1 catheter toward skin	4.10	3.44	3.43	25.6	48.4
4	3.0	3.0	7.0	10.0	1 catheter toward skin	4.10	3.44	3.43	25.6	39.4
5	3.0	3.0	5.0	10.0	1 catheter toward skin	4.10	3.44	3.43	25.6	33.7
6	3.0	5.0	10.0	10.0	1 catheter toward skin	4.10	3.44	3.43	25.6	51.0
7	3.0	5.0	7.0	10.0	1 catheter toward skin	4.10	3.44	3.43	25.6	41.9
8	3.0	5.0	5.0	10.0	1 catheter toward skin	4.10	3.44	3.43	25.6	36.3

Table 4.3.A: Optimized plans results – Part 1

Plan #	PTV thickness toward the				Max Skin Dose		Max CW Dose		Coverage Index (fraction of PTV Est receiving at least 340 cGy) = V100 (%)	Fraction of PTV Est receiving at least 323 cGy = V95 (%)
	Skin (mm)	CW (mm)	(+)90° & (-)90° from Skin (mm)	Shaft & Tip (mm)	(cGy)	(% of Rx dose)	(cGy)	(% of Rx dose)		
Limit					*≤ 425*	*≤ 125*	*≤ 425*	*≤ 125*	*N/A*	*N/A*
1	10.0	10.0	10.0	10.0	344.8	**101.4**	350.5	**103.1**	98.00	99.31
2	5.0	5.0	5.0	10.0	346.1	**101.8**	354.6	**104.3**	97.44	99.12
3	3.0	3.0	10.0	10.0	408.0	**120.0**	408.0	**120.0**	80.85	85.91
4	3.0	3.0	7.0	10.0	408.0	**120.0**	408.0	**120.0**	94.23	97.81
5	3.0	3.0	5.0	10.0	408.0	**120.0**	408.0	**120.0**	99.86	99.98
6	3.0	5.0	10.0	10.0	408.0	**120.0**	408.0	**120.0**	86.03	90.98
7	3.0	5.0	7.0	10.0	408.0	**120.0**	408.0	**120.0**	98.28	99.91
8	3.0	5.0	5.0	10.0	350.5	**103.1**	366.5	**107.8**	97.98	99.75

Table 4.3.B: Optimized plans results – Part 2

Plan #	PTV thickness toward the				Fraction of PTV Est receiving at least 306 cGy = V90 (%)	% of the Rx dose delivered to 90% of the PTV = D90 (%)	V150 (volume of tissue receiving at least 150% of the Rx dose)		V200 (volume of tissue receiving at least 200% of the Rx dose)	
	Skin (mm)	CW (mm)	(+)90° & (-)90° from Skin (mm)	Shaft & Tip (mm)			(cc)	(%)	(cc)	(%)
Limit					*≥ 90*	*≥ 90*	*≤ 50*	*N/A*	*≤ 10*	*N/A*
1	10.0	10.0	10.0	10.0	**99.70**	104.92	**27.06**	38.49	**9.10**	12.94
2	5.0	5.0	5.0	10.0	**99.58**	103.85	**9.46**	24.38	**2.67**	6.88
3	3.0	3.0	10.0	10.0	**90.44**	90.53	**12.44**	25.71	**4.40**	9.10
4	3.0	3.0	7.0	10.0	**99.75**	104.33	**11.97**	30.39	**4.08**	10.35
5	3.0	3.0	5.0	10.0	**100.00**	113.83	**11.91**	35.35	**4.07**	12.07
6	3.0	5.0	10.0	10.0	**95.00**	96.05	**15.06**	29.53	**4.28**	8.39
7	3.0	5.0	7.0	10.0	**99.99**	108.46	**14.51**	34.64	**3.90**	9.31
8	3.0	5.0	5.0	10.0	**99.95**	105.54	**9.81**	27.03	**3.23**	8.90

Table 4.3.C: Optimized plans results – Part 3

Plan #	PTV thickness toward the				PTV Est					PTV Evl				
	Skin (mm)	CW (mm)	(+)90° & (-)90° from Skin (mm)	Shaft & Tip (mm)	V300 (volume of tissue receiving at least 300% of the Rx dose)		PTV Est Min, Max & Mean doses as % of Rx dose			V300 (volume of tissue receiving at least 300% of the Rx dose)		PTV Evl Min, Max & Mean doses as % of Rx dose		
					(cc)	(%)	Min	Max	Mean	(cc)	(%)	Min	Max	Mean
Limit					*N/A*	*N/A*	*N/A*	*N/A*	*N/A*	*N/A*	*N/A*	*N/A*	*N/A*	*N/A*
1	10.0	10.0	10.0	10.0	**0.11**	0.16	76.0	**385.7**	147.2	**0.26**	0.36	73.7	**535.0**	148.0
2	5.0	5.0	5.0	10.0	**0.25**	0.64	74.7	**435.3**	137.2	**0.64**	1.59	71.0	**788.5**	140.6
3	3.0	3.0	10.0	10.0	**0.81**	1.67	70.8	**517.7**	136.6	**1.36**	2.73	70.7	**830.2**	140.6
4	3.0	3.0	7.0	10.0	**0.69**	1.75	86.7	**489.8**	145.0	**1.22**	2.99	82.3	**806.5**	149.4
5	3.0	3.0	5.0	10.0	**0.69**	2.05	91.6	**489.4**	152.2	**1.21**	3.45	82.4	**806.9**	156.9
6	3.0	5.0	10.0	10.0	**0.62**	1.22	77.4	**471.1**	139.1	**1.21**	2.31	77.2	**784.5**	142.4
7	3.0	5.0	7.0	10.0	**0.50**	1.19	86.7	**444.2**	146.6	**0.97**	2.24	78.1	**778.0**	150.0
8	3.0	5.0	5.0	10.0	**0.48**	1.32	83.1	**455.4**	141.3	**0.97**	2.58	76.1	**886.9**	145.8

Table 4.3.D: Optimized plans results – Part 4

The required limits for all required parameters were achieved in all 16 plans even though in some scenarios the evaluation parameters were close to the edge of acceptability. Larger the difference between the thickness of the PTV (Evl or Est) in the Anterior (Skin) to Posterior (Chest Wall) direction compared to the thickness in the Left [(+) 90°] to Right [(-) 90°] direction, more difficult is to achieve a high Coverage Index (V100), V95, V90 and D90 while keeping the Max Dose to Skin, Max dose to Chest Wall, V200 and V150 in the required limits. The most difficult cases to plan were Plan #6 and especially Plan #3, due to the close proximity to the skin and Chest Wall of the PTV expansion.

The author tried to emphasize the difference between the required and relevant parameters, as well as the limiting factors followed during the planning and optimization process. Therefore, the required limits of the required parameters are shown in the tables 4.2. under Limit, in Bold Red characters. The most significant data from the plans in tables 4.3. are shown in Bold Blue characters (required) or Bold Black characters (important).

Tables 4.3.A., 4.3.B. and 4.3.C. are showing the results for the plans in which PTV Est was used. The results for the plans in which PTV Evl was used are very close to the ones shown.

Table 4.3.D. shows the results for V300 and the Minimum, Maximum and Mean Dose in the PTV when the PTV Est and the PTV Evl were used in planning. As we can see, V300 is always better when using PTV Est. The Maximum Dose in the PTV is by far better when PTV Est was used in planning. This is due to the fact that the PTV thickness in the direction of the central catheter (Head to Feet) was always 10mm, forcing the high isodose lines (200%) to penetrate pretty deep into the PTV. But in these areas, the structures getting the highest doses are actually not tissue but the Tip and the Shaft of the central catheter of the MS-ML. This is why the recommendation is to use the PTV Est rather than the PTV Evl, especially when the Maximum Dose in the PTV Evl is high.

CONCLUSIONS

As pointed out throughout this thesis, the rationale for this study was to determine the optimal option for a device utilized in Accelerated Partial Breast Irradiation that would provide increased flexibility in regard to patient selection as well as to planning aspects. The existing Mammosite device, which had been successfully utilized since 2000 to treat early stage breast cancers following breast conserving surgery with High Dose Rate Brachytherapy has several limitations. This situation led to the impetus for the development of a new type of device that would accommodate a larger patient selection and that would also provide a superior dose distribution over the planning target volume. One of the main disadvantages of the classical Mammosite balloon was due to the fact that it only had a single central channel, therefore the therapeutical dose could only be delivered with the same intensity all around the inflated balloon. In clinical practice this constraint was sometimes challenging, due to the asymmetrical inflation of some of the balloons, or due to the proximity of the skin and/or chest wall, risking to create hot spots at the skin or chest wall level. In an effort to eliminate these constraining factors, ten new multichannel balloon based prototype devices were tested for dosimetric efficacy, flexibility, and complexity of dose distribution, and also to facilitate an improved clinical implementation.

The current research consisted in the testing of ten prototype devices under three potential clinical situations following three alternative sets of planning criteria. As a result I developed 52 treatment plans. From all the 10 test articles I generated treatment plans that met all the reference criteria (CI, D90, Max Dose to skin, V150, V200, EI).

All the reference criteria were clearly achieved by each of the test devices and met the requirements previously defined for all planning criteria. This shows that each of the 10 tested devices is at least as effective dosimetrically as any MS of the same balloon size. Also, each of the test devices can better spare the skin than any symmetrical MS of the same balloon size. Furthermore, in some extreme scenarios, all the tested balloons can drastically reduce the dose to the skin, while also meeting all the reference criteria. This was not achievable for any of the symmetrical MS. All 10 of the MSML test devices are dosimetrically superior to the symmetrical MS of the same balloon size.

I conclude that the best prototype device among the ten balloons studied in this research is test device #1, as it proved to have the optimum configuration for an MS-ML to be used in Accelerated Partial Breast Irradiation.

For the clinical situations when the use of a balloon type device is limited by the geometrical location of the tumor, a parallel study was developed, where the balloon was minimally inflated, to a volume of 23 cc. In this scenario 8 clinical situations were considered for planning, assuming that the closest distance to the skin and to the chest wall were in a plane orthogonal to the MS-ML lumens and passing through the center of the MS-ML balloon. PTV Evl and PTV Est were created considering two scenarios: the plastic (non-tissue) areas located outside the balloon and containing the catheters (tip and shaft) were either subtracted or not from the PTV. A number of 16 plans, 8 for each of the scenarios were developed and the dosimetrical requirements were defined. Following the process of structure reconstruction, planning, and optimization the following parameters were evaluated using DVHs: PTV size, Max Skin Dose, Max Chest Wall Dose, V100, V95, V90, D90, V150, V200, V300 and the Min, Max, and Mean Dose in the PTV.

The limits required of all the defined parameters were achieved in all of the 16 plans, even though in some scenarios the evaluation parameters were close to the edge of acceptability.

In all of the 16 plans, the reference criteria defined for all the potential clinical situations were met. The simplest case was Plan #1 and the most complex was Plan # 3. I recommend the use of PTV Est rather than PTV Evl, especially when the Maximum Dose in the PTV Evl is high. If the Maximum Dose in the PTV Evl remains high, the coverage of the PTV Est toward the Tip and toward the Shaft has to be diminished.

At least for the scenarios described in this study, the MS-ML device inflated using only 23cc of fluid can achieve all the required limits of all the required parameters for clinical use by taking advantage of some or all of the 4 available lumens in planning.

As a general conclusion I argue that a multilumen balloon type device (MS-ML) is dosimetrically superior to a single lumen balloon, and should be used clinically especially in challenging situations, where the breast size, the location of the tumor and its size, as well as the asymmetry of the balloon would be limiting factors for the use of Mammosite for Accelerated Partial Breast Irradiation [71].

Finally, as a direct result of this research, a prototype of the device indicated in this study as being optimal in terms of dosimetrical effectiveness and of sparing the organs at risk, was developed and launched by Hologic (Hologic, Inc., Bedford, MA), and is being successfully used in clinical practice in the United States since 2010.

ACKNOWLEDGMENTS

I am deeply indebted to my dissertation chair, Professor Dr. Onuc Cozar who recruited me in the program and has worked with me extensively to develop my research. Professor Cozar provided mentorship and support throughout the program. I owe special gratitude to my co-author, Dr. Stefan Both from the University of Pennsylvania who worked closely with me and provided in-depth discussions and guidance on how to improve my work. His constructive advice was very useful in developing my ideas. I am grateful to Dr. Marius Alecu from AROS LLC in Texas and Dr. Jeff Dorton from Hologic Inc., Massachusetts for helpful guidance and constructive feedback and for the opportunity to work on this project. In closing I would like to thank my entire family, especially my sister Georgiana, my husband Ciprian and my son Christian, for their support throughout the program.

SELECTED REFERENCES

1. American Cancer Society. Cancer Facts & Figures 2013. Atlanta: American Cancer Society; 2013.
2. World Health Organization. Cancer Fact Sheet No. 297; January 2013.
3. Fisher, B.; Anderson, S.; Redmond, C.K.; Wolmark, N.; Wickerham, L.; Cronin, W. M. Reanalysis and results after 12 years of follow-up in a randomized clinical trial comparing total mastectomy with lumpectomy with or without irradiation in the treatment of breast cancer. *N Engl J Med.* 333:1456-1461; 1995.
4. Vicini, F.; Kini, V.R.; Chen, P.; Horwitz, E.; Gustafson, G.; Benitez, P.; Edmundson, G., Goldstein, N.; McCarthy, K.; Martinez, A. Irradiation of the tumor bed alone after lumpectomy in selected patients with early-stage breast cancer treated with breast conserving therapy. *J Surg Oncol.* 70:33-40; 1999.
5. Baglan, K.L.; Martinez, A.A.; Frazier, R.C.; Kini, V.R.; Kestin, L.L; Chen, P.Y.; Edmundson, G.; Mele, E.; Jaffray, D.; Vicini, F.A. The use of high-dose rate brachytherapy alone after lumpectomy in patients with early-stage breast cancer treated with breast-conserving therapy. *Int J Radiat Oncol Biol Phys*. 50:1003-1011; 2001.
6. Vicini, F.A.; Chen, P.Y.; Fraile, M.; Gustafson, G.S.; Edmundson, G.K.; Jaffray, D.A.; Benitez, P.; Pettinga, J.; Madrazo, B.; Ingold, J.A.; Goldstein, N.S.; Matter, R.C.; Martinez, A.A. Low-dose-rate brachytherapy as the sole radiation modality in the management of patients with early stage breast cancer treated with breast conserving therapy: Preliminary results of a pilot trial. *Int J Radiat Oncol Biol Phys.* 38:301-310; 1997.
7. Vicini, F.A.; Kestin, L.L.; Edmundson, G.K.; Jaffray, D.A.; Wong, J.W.; Kini, V.R.; Chen, P.Y.; Martinez, A.A. Dose-volume analysis for quality assurance of interstitial brachytherapy for breast cancer. *Int J Radiat Oncol Biol Phys*. 45:803-810; 1999.
8. Kestin, L.L.; Jaffray, D.A.; Edmundson, G.K.; Martinez, A.A.; Wong, J.W.; Kini, V.R.; Chen, P.Y.; Vicini, F.A. Improving the dosimetric coverage of interstitial high-dose-rate breast implants. *Int J Radiat Oncol Biol Phys.* 46:35-43; 2000.
9. Fentiman, I.S.; Poole, C.; Tong, D.; Winter, P.J.; Gregory, W.M.; Mayles, H.M.O.; Turner, P.; Chaudary, M.A.; Rubens, R.D. Inadequacy of iridium implant as sole radiation treatment for operable breast cancer. *Eur J Cancer*. 32A:608-611; 1996.
10. Benitez, P.R.; Chen, P.Y.; Vicini, F.A.; Wallace, M.; Kestin, L.; Edmundson, G.; Gustafson, G.; Martinez, A. Partial breast irradiation in breast-conserving therapy by way of interstitial brachytherapy. *Am J Surg*. 188:355-364; 2004.

11. Baglan, K.L.; Sharpe, M.B.; Jaffray, D.; Frazier, R.C.; Fayad, J.; Kestin, L.L.; Remouchamps, V.; Martinez, A.A.; Wong, J.; Vicini, F.A. Accelerated partial breast irradiation using 3D conformal radiation therapy (3D-CRT). *Int J Radiat Oncol Biol Phys.* 55:302-311; 2003.

12. Vicini, F.A.; Remouchamps, V.; Wallace, M.; Sharpe, M.; Fayad, J.; Tyburski, L.; Letts, N.; Kestin, L.; Edmundson, G.; Pettinga, J.; Goldstein, N.S.; Wong, J. Ongoing clinical experience utilizing 3D conformal external beam radiotherapy to deliver partial breast irradiation in patients with early stage breast cancer treated with breast conserving therapy. *Int J Radiat Oncol Biol Phys.* 57:1247-1253; 2003.

13. Intra, M.; Gatti, G.; Luini, A.; Galimberti, V.; Veronesi, P.; Zurrida, S.; Frasson, A.; Ciocca, M.; Orecchia, R.; Veronesi, U. Surgical technique of intraoperative radiotherapy in conservative treatment of limited stage breast cancer. *Arch Surg*. 137:737-740; 2002.

14. Vaidya, J.S.; Tobias, J.S.; Baum, M.; Keshtgar, M.; Joseph, D.; Wenz, F.; Houghton, J.; Saunders, C.; Corica, T.; D'Souza, D.; Sainsbury, R.; Massarut, S.; Taylor, I.; Hilaris, B. Intraoperative radiotherapy for breast cancer. *Lancet Oncol*. 5:165-173; 2004.

15. Edmundson, G.K.; Vicini, F.A.; Chen, P.Y.; Mitchell, C.; Martinez, A.A. Dosimetric Characterisitics of the MammoSite RTS, a new breast brachytherapy applicator. *Int J Radiat Oncol Biol Phys.* 52:1132-1139; 2002.

16. Keisch, M.; Vicini, F.; Kuske, R.R.; Hebert, M.; White, J.; Quiet, C.; Arthur, D.; Scroggins, T.; Streeter, O. Initial clinical experience with the MammoSite breast brachytherapy applicator in women with early stage breast cancer treated with breast conserving therapy. *Int J Radiat Oncol Biol Phys.* 55:289-293; 2003.

17. Dickler, A.; Kirk, M.; Choo, J.; Hsi, W.C.; Chu, J.; Dowlatshahi, K.; Francescatti, D.; Nguyen, C. Treatment volume and dose optimization of MammoSite breast brachytherapy applicator. *Int J Radiat Oncol Biol Phys.* 59:469-474; 2004.

18. Chao, K.K.; Vicini, F.A.; Wallace, M.; Mitchell, C.; Chen, P.; Ghilezan, M.; Gilbert, S.; Kunzman, J.; Benitez, P.; Martinez, A. Analysis of treatment efficacy, cosmesis, and toxicity using the MammoSite breast brachytherapy catheter to deliver accelerated partial-breast irradiation: the William Beaumont Hospital experience. *Int J Radiat Oncol Biol Phys.* 69:32-40; 2007.

19. Cuttino, L.W.; Arthur, D.W.; Keisch, M.; Jenrette, J.M.; Prestidge, B.R.; Quiet, C.A.; Vicini, F.A.; Rescigno, J.; Wazer, D.E.; Patel, R. Multi-institutional experience using the MammoSite Radiation Therapy System (RTS) in the treatment of early-stage breast cancer:2 year results [Abstract]. *Int J Radiat Oncol Biol Phys.* 66:S30-S31; 2006.

20. Harper, J.L.; Jenrette, J.M.; Vanek, K.N.; Aguero, E.G.; Gillanders, W.E. Acute complications of mammosite brachytherapy: A single institution's initial clinical experience. *Int J Radiat Oncol Biol Phys.* 61:169-174; 2005.

21. Benitez, P.R.; Keisch, M.E.; Vicini, F.; Stolier, A.; Scroggins, T.; Walker, A.; White, J.; Hedberg, P.; Hebert, M.; Arthur, D.; Zannis, V.; Quiet, C.; Streeter, O.; Silverstein, M. Five-year results: the initial clinical trial of mammosite balloon brachytherapy for partial breast irradiation in early-stage breast cancer. *Am J Surg.* 194:456-462; 2007.

22. Prestidge, B.; Sadeghi, A.; Rosenthal, A.; Salinas, L.; Zubyk, S. Local control of early stage breast cancer using MammoSite HDR brachytherapy [Abstract]. *Int J Radiat Oncol Biol Phys.* 66:S215; 2006.

23. Yashar, C.; Scanderberg, D.; Kuske, R.; Wallace, A.; Zannis, V., Blair, S.; Grade, E.; Swenson, V.H.; Quiet, C. Initial clinical experience with the strut-adjusted volume implant (SAVI) breast brachytherapy device for accelerated partial-breast irradiation (APBI): first 100 patients with more than 1 year of follow-up. *Int J Radiat Oncol Biol Phys* 2010; DOI: 10.1016/j/ijrobp.2010.018.

24. Cross, C.; Brown, A.; Escobar, P.; Kokal, W.; Mantz, C. Partial breast brachytherapy utilizing the single-entry, multicatheter SAVI device in patients with less than 7 mm skin-to-cavity distance: favorable acute skin toxicity outcomes from a phase II trial [Abstract]. *Int J Radiat Oncol Biol Phys.* 72:S182; 2008.

25. Gurdalli, S.; Kuske, R.; Quiet, C.A.; Howard, V. Dosimetric performance of SAVI: A new single-entry, multi-catheter breast brachytherapy applicator. *Brachytherapy.* 7:142-143; 2008.

26. Scanderberg, D.J.; Yashar, C.; Rice, R.; Pawlicki, T. Clinical implementation of a new HDR brachytherapy device for partial breast irradiation. *Radiother Oncol*. 90:36-42; 2009.

27. Cuttino, L.W.; Todor, D.; Rosu, M.; Arthur, D.W. Skin and chest wall dose with multi-catheter and MammoSite breast brachytherapy: Implications for late toxicity. *Brachytherapy*. 8:223-226; 2009.

28. Arthur, D.W.; Vicini, F.A.; Todor, D.A., Julian, T.B.; Lyden, M.R. Improvements in critical dosimetric endpoints using the Contura Multilumen Balloon breast brachytherapy catheter to deliver accelerated partial breast irradiation: Preliminary dosimetric findings of a phase IV trial. *Int J Radiat Oncol Biol Phys*. 79:26-33; 2011.

29. Brown, S.; McLaughlin, M.; Pope, K.; Haile, K.; Hughes, L.; Israel, P.Z. Initial radiation experience evaluating early tolerance and toxicities in patients undergoing accelerated partial breast irradiation using the Contura multi-lumen balloon breast brachytherapy catheter. *Brachytherapy.* 8:227-233; 2009.

30. Wilder, R.B.; Curcio, L.D.; Khanijou, R.K.; Eisner, M.E.; Kakkis, J.L.; Chittenden, L.; Agustin, J.; Lizarde, J.; Mesa, A.V.; Ravera, J.; Tokita, K.M. A Contura catheter offers dosimetric advantages over a MammoSite catheter that increase the applicability of accelerated partial breast irradiation. *Brachytherapy.* 8:373-378; 2009.

31. Hendee, E.G.; Ibbott, G.S.; Hendee, W.R. Radiation Therapy Physics, 3rd Edition. Published by *John Wiley & Sons Inc.*; 2004

32. Podgorsak, E.B. Radiation Physics for Medical Physicists. Published by *Springer Verlag*; 2010.

33. Hendee, W.R. Medical Radiation Physics. Published by *Year Book Medical Publishers*; 1973.

34. Johns, H.E.; Cunningham, J.R. The Physics of Radiology, 4th Edition. Published by *Charles C. Thomas Publisher*; 1983.

35. Khan, F.M. The Physics of Radiation Therapy, 4th Edition. Published by *Lippincott Williams & Wilkins*; 2010.

36. Khan, F.M. The Physics of Radiation Therapy, 3rd Edition. Published by *Lippincott Williams & Wilkins*; 2003.

37. Nag, S. High Dose Rate Brachytherapy. Published by *Futura Publishing Company Inc*.; 1994.

38. Henske, U.K.; Hilaris, B.S.; Mahan, G.D. Remote afterloading for intracavitary radiation therapy. In Ariel IM, Ed. Progress in Clinical Cancer. Published by Grune&Stratton, NY; 1965.

39. Henske, U.K.; Hilaris, B.S.; Mahan, G.D. Remote afterloading with intracavitary applicators. *Radiology*. 83 (2):344-345; 1964.

40. Walstam, R. Remotely controlled afterloading apparatus. *Acta Radiol (Ther)* Suppl 236, Part II, 84, 1965.

41. **Stan, A**. New advances and techniques used in Accelerated Partial Breast Irradiation. Presented at the *5th Edition of State of the Art in Radiation Therapy*, Dallas, TX, USA; December 9-11, 2011.

42. **Stan, A**. High Dose Rate Brachytherapy – planning challenges for breast applicators. Presented at the *5th Edition of State of the Art in Radiation Therapy*, Dallas, TX, USA; December 9-11, 2011

43. Kubo, H.D.; Glasgow, G.P.; Pethel, T.D.; Thomadsen, B.R.; Williamson, J.F. High dose rate brachytherapy treatment delivery: Report of the AAPM Radiation Therapy Committee Task Group No. 59. *Med. Phys*. 25 (4); 1998.

44. Nath, R.; Anderson, L.L.; Jones, D.; Ling, C.; Loevinger, R.; Williamson, J.; Hanson, W. Specification of brachytherapy source strength: Report of the AAPM Radiation Therapy Committee Task Group No. 43. American Association of Physicists in Medicine; American Institute of Physics New York, NY; 1987.

45. Nath, R.; Anderson, L.L.; Luxton, G.; Weaver, K.A.; Williamson, J.F.; Meigooni, A.S. Dosimetry of Interstitial Brachytherapy: Report of the AAPM Radiation Therapy Committee Task Group No. 32. New York, NY: American Institute of Physics; 1995.

46. Nath, R.; Anderson, L.L.; Luxton, G.; Weaver, K.A.; Williamson, J.F.; Meigooni, A.S. Dosimetry of Interstitial Brachytherapy: Report of the AAPM Radiation Therapy Committee Task Group No. 32. New York, NY: American Institute of Physics; 1995.

47. Rivard, M.J.; Coursey, B.M.; DeWerd, L.A.; Hanson, W.F.; Huq, M.S.; Ibbott, G. S.; Mitch, M.G.; Nath, R.; Williamson, J.F. Update of AAPM Task Group No. 43 Report: A revised AAPM protocol for brachytherapy dose calculations. *Med. Phys*. 31 (3); 2004.

48. Beaulieu, L.; Tedgren, A.C.; Carrier, J.F.; Davis, S.D.; Mourtada, F.; Rivard, M.J.; Thomson, R.M.; Verhaegen, F.; Wareing, T.; Williamson, J.F. Report of the Task Group 186 on model-based dose calculation methods in brachytherapy beyond the TG-43 formalism: Current status and recommendations for clinical implementation. *Med. Phys*. 39 (10); 2012.

49. Glasgow, G.P.; Bourland, J.D.; Grigsby, P.W.; Meli, J.A.; Weaver, K.A. Remote afterloading technology. American Association of Physicists in Medicine Report 41. New York, NY: American Institute of Physics; 1993

50. United States Nuclear Regulatory Commission. Allan, J.R.; Kelley, R.T.; Quinn, M.L.; Gwynne, J.W.III; Moore, R.A.; Muckler, F.A.; Kasumovic, J.; Saunders, W.M.; Lepage, R.P.; Chin, E.; Schoenfield, I.; Serig, D.I. Human Factors Evaluation of Remote Afterloading Brchyterapy. *NUREG/CR-6125 (Vols. 1, 2 and 3),* United States Nuclear Regulatory Commission, Washington, D.C.; 1995.

51. Orton, C.G.; Bremer, D.J.; Dale, R.G.; Fowler, J.F. Radiobiology. In *Textbook on High Dose Rate Brachytherapy.* Edited by Nag, S.; Futura Publishing Company, Inc.,Armonk, N.Y.; 1994.

52. Hall, E.J.; Giaccia, A.J. Radiobiology for the Radiologist. Published by *Lippincott Williams & Wilkins*; 2011.

53. Barendsen, G.W. Dose fractionation, dose rate and iso-effect relationships for normal tissue responses. *Int J Radiat Oncol Biol Phys* 8:1981-1997; 1982.

54. Orton, C.G. Recent developments in time-dose modeling. *Australas Phys Eng Sci Med* 14:57-64, 1991.

55. Orton, C.G. High and low dose rate remote afterloading: a critical comparison. In *International Radiation Therapy Techniques - Brachytherapy*. Edited by Sauer, R.; Berlin, Germany: Springer-Verlag; 1991.

56. Fowler, J.F. The linear-quadratic formula and progress in fractionated radiotherapy. *Brit J Radiol* 62:679-694; 1989.

57. Podgorsak, M.B.; DeWerd, L.A.; Paliwal, B.R. The half-life of high dose rate Ir-192 source. *Med Phys*. 20, 1257-1259; 1993.

58. Both, S.; Alecu, J.; **Stan, A.**; Alecu, M.; Ciura, A.; Hansen, J.; Alecu, R. A study to establish reasonable action limits for patient specific IMRT QA. *Journal of Applied Clinical Medical Physics*, 8 (2), 1-8; 2007.

59. **Stan, A.**; Cernea, V. Quality Assurance and Quality Control in Clinical Dosimetry ad Radiotherapy. Presented at the 9th Balkanic Congress of Oncology, Poiana Brasov, Romania; 2000.

60. Goetsch, S.J.; Attix, F.H.; Pearson, D.W.; Thomadsen, B.R. Calibration of ^{192}Ir high-dose rate afterloading systems. *Med. Phys*. 18 (3); 1991

61. Goetsch, S.J.; Attix, F.H.; DeWerd, L.A. A new well ionization chamber for the calibration of Iridium-192 high dose rate sources. *Int J Radiat Oncol Biol Phys* 24, 167-170; 1992.

62. Schoeppel, S.L.; Lavigne, M.L.; Mantel, M.K. Three dimensional treatment planning of intercavity gynecologic implants analysis of ten cases and implications for dose specification. *Int J Radiat Oncol Biol Phys* 28*,* 277-283; 1993.

63. Weeks, K.J. brachytherapy object-oriented treatment planning based on three dimensional image guidance. In *Categorical course in brachytherapy physics.* Edited by Thomadsen, B; Radiological Society of North America; Oak Brook, IL; 1997.

64. Wang, R.; Sloboda, R.S. Monte Carlo dosimetry of the VariSource high dose rate ^{192}Ir source. *Med. Phys.* 25, 415-423; 1998.

65. Cernea, D.; Kacso, G.; **Stan, A**. Radio Chemotherapy in High Grade Gliomas. The experience of Oncology Institute Cluj 1995-2001. *Journal of Radiotherapy and Medical Oncology*, Vol. IX, Nr.1; 17-23; 2003.

66. Cudalbu, C.; **Stan, A**.; Cozar, O.; Ristoiu, D. Dose distribution in the irradiation of medulloblastoma with two adjacent fields. Studia UBB, Physica, Issue; 48(2), 3-11; 2003.

67. **Stan, A**. Intensity Modulated Radiation Therapy – essential planning aspects for pelvic and thoracic organs. Presented at the 6th Edition of *State of the Art in Radiation Therapy*. Colleyville, TX, USA. December 7-9; 2012.

68. **Stan, A**. Intensity Modulated Radiation Therapy vs. High Dose Rate Brachytherapy in the treatment of breast cancers. Presented at the 4th Edition of *State of the Art in Radiation Therapy*. Dallas, TX, USA. October 20-23; 2010.

69. NSABP Protocol B-39, RTOG Protocol 0413.

70. Wazer, D.E.; Lowther, D.; Boyle, T.; Ulin, K.; Neuschatz, A.; Ruthazer, R.; DiPetrillo, T.A. Clinically evident fat necrosis in women treated with high-dose-rate brachytherapy alone for early-stage breast cancer. *Int J Radiat Oncol Biol Phys*. 50:107-111; 2001.

71. **Stan, A.R**; Alecu, M.; Alecu, R.; Both, S.; Cozar, O. A MammoSite Multilumen (MS-ML) balloon used for accelerated partial breast irradiation. *Rom. Journ. Phys*., 58 (1-2), 117-126; 2013.

72. Wazer, D.E.; Kaufman, S.; Cuttino, L.; DiPetrillo, T.; Arthur, D.W. Accelerated partial breast irradiation: An analysis of variables associated with late toxicity and long-term cosmetic outcome after high-dose-rate interstitial brachytherapy. *Int J Radiat Oncol Biol Phys*. 64:489-495, 2006.